Northumbria University
NEWCASTLE

University**Library**

International Communications in Heat and Mass Transfer 124 (2021) 105244

Contents lists available at ScienceDirect

International Communications in Heat and Mass Transfer

journal homepage: www.elsevier.com/locate/ichmt

Optimizing the energy recovery section in thermal desalination systems for improved thermodynamic, economic, and environmental performance

Muhammad Ahmad Jamil [a,b], Talha S. Goraya [b], Kim Choon Ng [c], Syed M. Zubair [d], Ben Bin Xu [a], Muhammad Wakil Shahzad [a,c,*]

[a] Mechanical & Construction Engineering Department, Northumbria University, Newcastle Upon Tyne NE1 8ST, UK
[b] Department of Mechanical Engineering, Khwaja Fareed University of Engineering and Information Technology, Rahim Yar Khan, Pakistan
[c] Water Desalination and Reuse Centre, King Abdullah University of Science & Technology, 23955-6900 Thuwal, Saudi Arabia
[d] Mechanical Engineering Department, KFUPM Box # 1474, King Fahd University of Petroleum & Minerals, Dhahran 31261, Saudi Arabia

ARTICLE INFO

Keywords:
Plate heat exchangers
Preheaters
Desalination
Energy recovery
Genetic algorithm
Optimization
Economic analysis

ABSTRACT

Integration of energy recovery section with thermal desalination systems improves their performance from thermodynamics, economics, and environmental viewpoints. This is because it significantly reduces input energy, heat transfer area, and capital cost requirements. Above all, the system outlet streams can achieve thermal equilibrium with the environment by supplying heat for useful preheating purposes thus reducing the environmental impacts. The plate heat exchangers are generally employed for this purpose as preheaters. The current paper presents a comprehensive investigation and optimization of these heat exchangers for thermal desalination systems applications. An experimentally validated numerical model employing Normalized Sensitivity Analysis and Genetic Algorithm based cost optimization is developed to investigate their performance at assorted operating conditions. The analysis showed that the heat transfer coefficient, pressure drop, and outlet water cost were improved by an increase in feed flow rate. However, with an increased flow rate, the comprehensive output parameter (h/ΔP) decreased due to the high degree increase in pressure drop. Moreover, an increase in the chevron angle reduced the heat transfer coefficient, pressure drop, and water cost. Finally, the optimization lowered the heat transfer area by ~79.5%, capital investment by ~62%, and the outlet cost of the cold stream by ~15.7%. The operational cost is increased due to the increased pressure drop but the overall impact is beneficial as C_{total} of equipment is reduced by ~52.7%.

1. Introduction

Thermal-based desalination systems are the mainstay of the water treatment industry and share almost 40% globally [1]. These systems primarily include multistage flash (MSF) [2,3], multi-effect desalination (MED) [4,5], thermal/mechanical vapor compression (TVC/MVC) systems [6,7] and adsorption systems [8,9]. The prime reasons for their dominance are high operational reliability, the capability to handle harsh feeds, low pre-and post-treatment requirements, less maintenance/equipment-replacement expenses, and the ability to use low-grade energy [10–12]. However, these systems operate at high top brine temperature (i.e., $\geq$ 55 °C), and are regarded as energy and cost-intensive systems [13]. Therefore, substantial research has been conducted to improve their performance from thermodynamic and economic viewpoints [14–16]. One important development in this regard is the energy recovery i.e., preheating of intake by heat recovery from the distillate and brine streams [17]. This approach offers many advantages from thermodynamic, monetary, and environmental perspectives as it recovers heat that would be wasted otherwise resulting in higher thermal losses and increased risk for the aquatic life in the vicinity [18,19]. Moreover, it also reduces the sensible heating loads in the evaporators which lowers the area and investments [20].

The most commonly used preheaters for this purpose are the corrugated plate heat exchangers (PHXs) [21]. The salient features that make PHXs the most suitable for this job include narrow temperature control, easy maintenance, high operating reliability, and flexibility to accommodate varying loads [22,23]. However, it is important to mention that despite considerable importance, a cost-optimized design and analysis of PHXs as preheaters has seldom been conducted in desalination system studies [24–26]. Rather, the heat exchanger design is either missing [27] or restricted to preliminary sizing [28]. The heat transfer area in these

* Corresponding author at: Mechanical & Construction Engineering Department, Northumbria University, Newcastle Upon Tyne NE1 8ST, UK.
E-mail address: muhammad.w.shahzad@northumbria.ac.uk (M.W. Shahzad).

https://doi.org/10.1016/j.icheatmasstransfer.2021.105244

Available online 23 March 2021

Nomenclature

C_h	constant for Nusselt number calculation in Table 3
$\dot{C}$	product cost, ($/h)
C_{total}	total cost of equipment, $
C_o	annual current cost, $/y
C_{ele}	cost of electricity, $/kWh
$\overline{ex}$	Specific exergy, k.J/kg
h	local heat transfer coefficient, W/m^{2}K
h'	enthalpy, kJ
i	interest rate, %
$\dot{m}$	mass flow rate, kg/s
N_p	number of plates
Nu	Nusselt number
n_y	equipment life, year
PP	pumping power, W
ΔP	pressure drop, Pa
Pr	Prandtl number
Re	Reynolds number
s	Entropy, J/K
U	global heat transfer coefficient, W/m^{2}K
$\dot{W}_p$	pump work, kW
$\dot{X}$	flow exergy rate, kW
X_D	exergy destruction, kW
$\dot{Z}$	annual rate of capital investment, $/y

Greek symbols

ζ	rate of fixed cost, $/s
β	chevron angle, deg
Δ	change in quantity
∂	partial
ρ	density, kg/m^3
μ	viscosity, kg/ms
Λ	Operation hours, hour
η	efficiency
δ	local sensitivity
ζ_x	certainty about nominal value

Subscripts

0	dead state
B	brine
c	cold
ci	cold in
co	cold out
ch	per channel
h	hot
hi	hot in
ho	hot out
i	inlet
man	manifold
o	outlet
P	port
SW	Sea Water
t	total
w	wall

Superscripts

m	constant for friction factor calculation
n	constant for Nusselt number calculation
w	wall

Abbreviations

CRF	capital recovery factor
CAPEX	capital investment
CEPCI	chemical engineering plant cost index
ER	energy recovery
GOR	gain output ratio
HX	heat exchange
LMTD	log mean temperature difference
MED	multi-effect desalination
MSF	multistage flash
MVC	mechanical vapor compression
NSC	normalized sensitivity coefficients
PHXs	plate heat exchangers
OFAT	one-factor-at-a-time
OPEX	operational cost
RC	relative contribution
SEE	single effect evaporation
SEC	specific energy consumption
TVC	thermal vapor compression

studies is estimated using conventional heat transfer coefficient correlations that are only a function of temperature proposed by Dessouky et al. [29–31]. Though the methods give a quick estimate of the heat transfer area, the reliability of such calculations is suspected. This is because the heat transfer coefficients in heat exchangers are the functions of temperature, pressure, thermophysical properties, geometric constraints, and flow characteristics [32–34]. For instance, many studies reported the plate chevron angle (β) as the most important geometric parameter governing the thermodynamic performance of PHXs [35–39]. Similarly, flow rate, fluid properties, and heat duty also have a remarkable effect on thermohydraulic performance [40–42]. The optimization studies have also reported multiple geometric and process parameters that control the PHX performance [43–46]. The most influencing parameters have been identified as, number of plates/channels, plate type (pattern), dimensions of chevron corrugation, number of passes, type of channel flow [47–49].

The literature review suggests that there is a significant need for a rigorous cost-effective design and analysis of the energy recovery section for thermal desalination systems. One of the recent works partially addressing this issue is conducted by Jamil et al. [50]. However, the study presented the design and analysis of preheating section from a thermohydraulic viewpoint only and lacks economic analysis and optimization. The current paper is focused to add value by optimizing the thermal-hydraulic model (presented in [50]) for minimum cost. For this purpose, a very useful and reliable tool "Exergoeconomic Analysis" is employed as a simultaneous application of thermodynamics and monetary analyses. The study is designed to achieve the following objectives: (a) a detailed thermal-hydraulic design and analysis using experimentally validated numerical model, (b) Second Law analysis, (c) economic analysis for capital and operational cost, (d) sensitivity analysis for Normalized Sensitivity Coefficients (NSC) and Relative Contribution (RC) of sensitive parameters, (e) parametric analysis using a one-factor-at-a-time approach, and (f) optimization for minimum cost using Genetic Algorithm.

2. Impact of the energy recovery section

The layout of a traditional desalination system integrated with the energy recovery (ER) section is shown in Fig. 1. The ER section consists of two plate heat exchangers i.e., feed and brine preheaters based on the hot fluid stream. A recent study by Abid et al. [51,52] on the impacts of incorporating energy recovery section with a forward feed MED system conforms its benefits from thermodynamics, economic, and environmental perspectives. The analysis reported that for a 4-effect forward

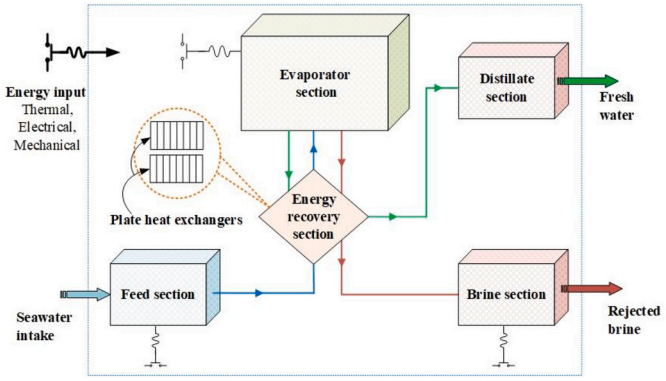

Fig. 1. Conventional thermal desalination system with energy recovery.

feed MED system, the ER section increased the feed temperature up to 35%. Consequently, the Gain Output Ratio (GOR) improved by 17.9%, the Specific Energy Consumption (SEC) decreased by 15% (refer Fig. 2 (a)) and the heat transfer area by reduced by 0.42%. The total exergy destruction and the water production cost are reduced by 5.5% and 10.5% (see Fig. 2 (b)) due to the reduction in heat transfer area and energy consumption. In addition, the temperatures of the distillate and brine streams are lowered by 45% and 50%, which is an added advantage from the environmental point of view (refer to Fig. 4). Therefore, critical analysis and cost-optimized design of the energy recovery section are essential to achieve the goals of minimum water production cost. (See Fig. 3.)

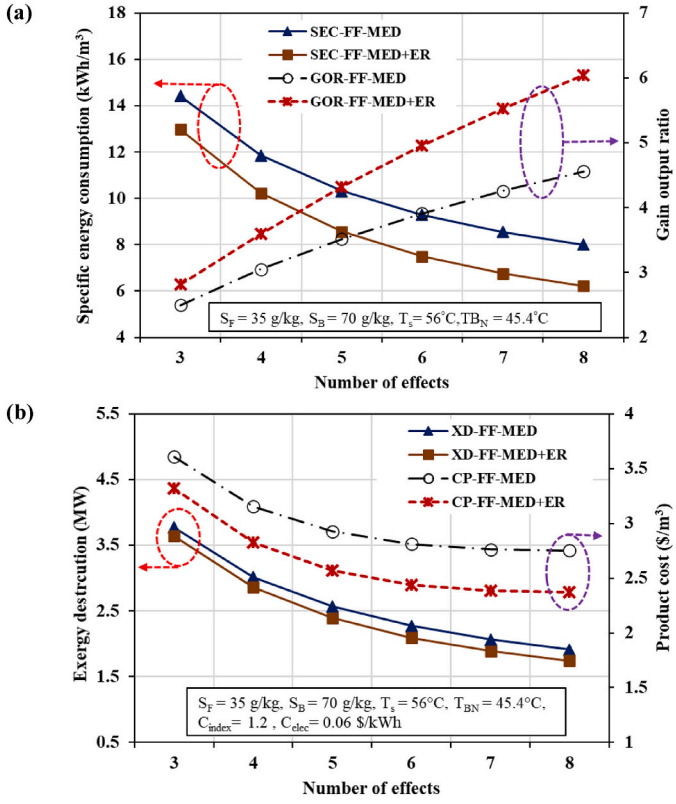

Fig. 2. Impact of energy recovery on the thermodynamic and economic performance of forward feed MED system.

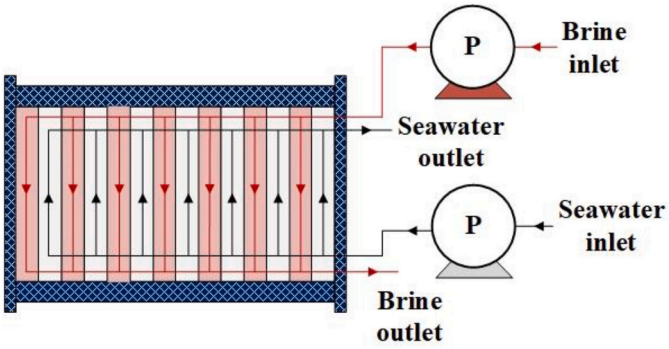

Fig. 4. The schematic diagram for heat exchanger configuration.

3. Materials and methods

3.1. Heat exchanger configuration

The system under consideration consists of a corrugated plate heat exchanger and two pumps to manage the desired flow rates and pressures as shown in Fig. 4. The system preheats the intake seawater using a hot brine stream coming from a Single Effect Mechanical Vapor Compression (MVC) based thermal desalination system [53]. The operating parameters i.e., temperatures, mass flows, and salinity of cold and hot streams are taken from recent studies for a practical design and analysis purpose as summarized in Table 1 [53].

3.2. Thermal-hydraulic analysis model

The thermal-hydraulic design presented in [50] is used for the calculation of temperatures, flow rates, heat duty, local and overall heat transfer coefficients, heat transfer area, pressure drops, and pumping power. The thermal analysis involves the calculation of the Nusselt number (*Nu*) which is given as a function of Reynold number (*Re*) and Prandtl number (*Pr*) [54–56].

$$Nu = C_h Re^n \; Pr^{\frac{1}{3}} \left(\frac{\mu}{\mu_w}\right)^{0.17} \tag{1}$$

where C_h and n vary with Re and β as given in [50,54–56].

The hydraulic design involves the calculation of total pressure drop which is the sum of the pressure drop in channels, ports, and manifolds as given [39,56].

$$\Delta P_{total} = \Delta P_{ch} + \Delta P_p + \Delta P_{man} \tag{2}$$

The pumping power, which is the main parameter governing the operational cost of the heat exchanger is calculated as.

$$P_{power} = \frac{\dot{m}\,\Delta P_{total}}{\eta \rho} \tag{3}$$

A detailed discussion regarding the selection and implementation of these correlations is presented in the referred study [50].

3.3. Exergy analysis

It is an important tool for heat exchanger optimization because it involves the calculation of lost work (exergy destruction) [57]. This is because the desirable high heat transfer coefficients in HXs are accompanied by corresponding high-pressure drops. The exergy analysis accounts for the variations in temperature and pressure simultaneously thus measuring overall performance. The performance index for this analysis is exergy destruction [58,59]. To conduct this analysis, the flow exergy is calculated at each terminal point (i.e., inlets and outlets of the pumps and HX) based on the mass flow rate salinity, temperature, and

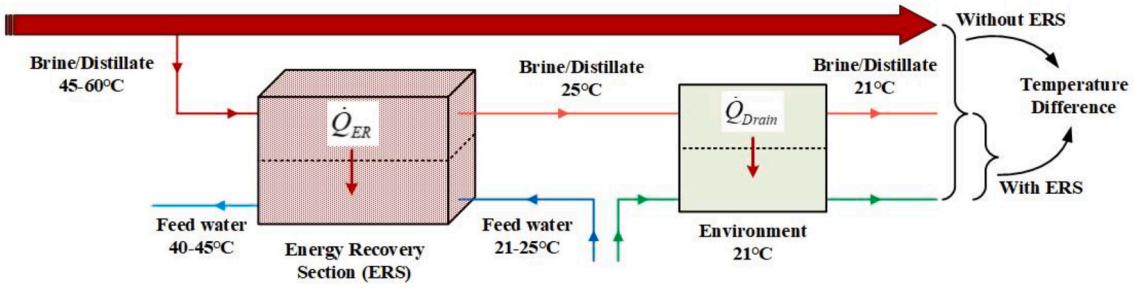

Fig. 3. Energy recovery from outlet streams for thermal equilibrium.

Table 1
Process input parameters [53].

Parameter	Value
Cold water flow rate, $\dot{m}_{SW}$(kg/s)	13
Hot water flow rate, $\dot{m}_B$(kg/s)	13
Coldwater temperature, T_{SW}(i/o) (°C)	21/57
Hot water temperature, T_B(i/o) (°C)	63/23
Coldwater salinity, S_{SW}(i/o) (°C)	40
Hot water salinity, S_{SW}(i/o) (°C)	80

pressure as given in Eq. 5. After that, a standard exergy balance equation is solved for all the component to get X_D as given in Eq. 6. In the current study, the specific flow exergy $\overline{ex}$ is calculated using the seawater library [60,61].

$$\overline{ex} = [(h' - h_0') - T_0(s - s_0)] + \overline{ex}_{che} \tag{4}$$

$$\dot{X} = \dot{m}\,\overline{ex} \tag{5}$$

$$\dot{X}_{Des} = \dot{X}_i - \dot{X}_o \tag{6}$$

3.4. Economic analysis

For standalone heat exchangers, the economic analysis is generally restricted to the calculation of capital and operational expenses i.e., CAPEX and OPEX, respectively [62–64]. However, for a system analysis with multiple components e.g., desalination systems consisting of heat exchangers, evaporators, pumps, compressors, etc. the stream cost is far more important than merely CAPEX and OPEX [65]. This is because, in these systems, the heat exchanger performance depends upon the plant operating parameters, and thus the HX is designed to fulfill the plant requirements rather than simply optimum local performance [53,66]. The details regarding the different components of economic analysis are presented below.

3.4.1. Capital expenses

These capital expenses (CAPEX) measure the money expended in equipment purchasing at the time and location of the study. The best approach for the calculation of CAPEX is the use of empirical correlations developed by researchers after an extensive survey. This is because for a flexible and rigorous design and analysis the parameter-dependent cost can only accommodate the variations in process and design parameters conveniently [67]. Therefore, in the current study, the CAPEX for pumps and heat exchanger is calculated using reliable correlation [68]. In this regard, all the correlations reported in the literature and their applicability ranges for heat exchangers are summarized in Table 2. It can be observed that the capital cost for a pump is given in terms of flow rate, pressure differential, and efficiency. While for heat exchanger the capital cost correlations are based on the heat transfer area. An installation factor of 1.5–2.0 is also used to accurately predict the expenses required to make the heat exchanger functional at the point

Table 2
Correlations for calculation of CAPEX of equipment.

Correlation	Applicability range (SI)	Ref.
$CAPEX^{\$}_{P} = 13.92\ \dot{m}\ \Delta P^{0.55}\,(\eta/(1-\eta))^{1.05}$ (✓)	$2 \le \dot{m} \le 32, 1.8 \le e \le 9{,}100 \le \Delta P \le 6200$	[68]
$CAPEX^{\$}_{PHX} = 1000(12.86 + A^{0.8}) \cdot IF$ (✓)	N/A	[76]
$CAPEX^{\$}_{PHX} = 1839 \cdot IF \cdot A^{0.4631}$	$A^{Tit} \le 18.6m^2$, $P \le 10$ bar, $T \le 160^oC$	[77–79]
$CAPEX^{\$}_{PHX} = 781 \cdot IF \cdot A^{0.7514}$	$A^{Tit} \ge 18.6m^2$, $P \le 10$ bar, $T \le 160^oC$	
$CAPEX^{\$}_{PHX} = 1281 \cdot IF \cdot A^{0.4887}$	$A^{SS} \le 18.6m^2$, $P \le 10$ bar, $T \le 160^oC$	
$CAPEX^{\$}_{PHX} = 702 \cdot IF \cdot A^{0.6907}$	$A^{SS} \ge 18.6m^2$, $P \le 10$ bar, $T \le 160^oC$	
$CAPEX^{\$}_{PHX} = 635.14 \cdot A^{0.778}$	SS-CS	[49,80,81]
$CAPEX^{\$}_{PHX} = 1391 \cdot A^{0.778}$	Titanium	

(✓) currently used, Where, *IF* is the installation factor for PHX ranging 1.5–2.0 [77].

of utility. Moreover, the constants in the correlations vary with changing materials, however the general form for all the correlations is almost same.

It is important to mention that the use of the above-discussed correlations requires a reasonable adjustment to adapt to the monetary variation in the equipment purchasing costs over the years due to fiscal policy changes [69]. In this aspect, the most systematic approach is the use of the cost index factor (C_{index}) [70,71]. The C_{index} is computed using CEPCI index of the original/reference year and the present year as given below [72,73].

$$C_{index} = \frac{CEPCI_{current}}{CEPCI_{reference}} \tag{7}$$

$$CAPEX^{\$}_{current} = C_{index} \times CAPEX^{\$}_{reference} \tag{8}$$

Cindex 1.7 is determined in the current analysis based on $CEPCI_{1990}$ 390 [74] and $CEPCI_{2020}$ 650 [75]. Nevertheless, the influence of Cindex is, however, studied for a wide variety of values for detailed design and analysis purposes.

3.4.2. Operational expenses

The operational expenses (OPEX) are calculated using annual current cost C_o ($/y), component life, n_y (year), unit energy rate, C_{elec} ($/kWh), yearly interest rate, i (%), operating hours $\Lambda(h/y)$, and pump power PP (kW) as.

$$OPEX = \sum_{j=1}^{n_y} \frac{C_o}{(1+i)^{\,j}} \tag{9}$$

$$C_o = PP \times C_{elec} \times \Lambda \tag{10}$$

$$PP = \frac{1}{\eta}\left(\frac{\dot{m}_{SW}\,\Delta P_{SW}}{\rho_{SW}} + \frac{\dot{m}_{B}\,\Delta P_{B}}{\rho_{B}}\right) \tag{11}$$

where, $n_y = 10$ year, $\Lambda = 7000\ h/y$, $i = 10\%$, $C_{elec} = 0.09$ ($/KWh) and $\eta = 78\%$ [62].

Finally, the total cost is calculated as [62,63].

$$C_{total} = CAPEX + OPEX \tag{12}$$

3.4.3. Exergoeconomic analysis and cost flow

The hot water outlet cost is estimated by applying the general cost approach [53]. In this regard, the CAPEX calculated above is transformed into the yearly rate of capital cost $\dot{Z}(\$/y)$ through capital recovery factor (*CRF*) which is given as [66].

$$CRF = \frac{i \times (1+i)^{n_y}}{(1+i)^{n_y} - 1} \tag{13}$$

$$\dot{Z} = CRF \times CAPEX \tag{14}$$

Then the cost flow rate in seconds i.e. ζ (in $/s) is determined using the plant availability factor (Λ) [19].

$$\zeta = \frac{\dot{Z}}{3600 \times \Lambda} \tag{15}$$

Thereafter, the cost balance takes the form [82].

$$\dot{C}_o = \Sigma \dot{C}_i + \zeta \tag{16}$$

where $\dot{C}_o$ represents the monetary value of the local output stream, $\dot{C}_i$ the monetary value the inlet stream, and the component cost rate ζ.

The cost balance for pump and HX are given as:

$$\dot{C}_o = \dot{C}_i + C_{elec}\,\dot{W}_P + \zeta_P \tag{17}$$

$$\dot{C}_{c,o} = \dot{C}_{c,i} + \dot{C}_{h,i} - \dot{C}_{h,o} + \zeta_{PHX} \tag{18}$$

The intake cost of cold water is taken from reference [83]. Meanwhile, it is worth mentioning that the components with multiple outputs (i.e., HXs, evaporation effects, flashing stages, and RO trains, etc.,) need supplementary equations for the solution. For a system with "k" outputs, a "k-1" number of supplementary equations are needed [84]. The equality of the average cost of inlet and outlet streams is based on these Eqs. [85]. The auxiliary equation to solve the cost balance of PHX is given as:

$$\frac{\dot{C}_{B,i}}{X_{B,i}} - \frac{\dot{C}_{B,o}}{X_{B,o}} = 0 \tag{19}$$

3.4.4. Sensitivity analysis

The sensitivity analysis also used as uncertainty propagation analysis (in experiments) is a powerful tool to assess the response of the output parameter to the perturbations in input parameters [86,87]. Besides measuring the "goodness" of results, this analysis can also satisfactorily conduct malfunction diagnosis and design improvements by highlighting the most responsive parameters for subsequent research [88,89]. In this regard, partial derivative-based sensitivity analysis is one of the most useful methods [90]. In this technique, all independent variables are simulated as a sum of their nominal values and the disturbances/perturbations as below [91].

$$X = \overline{X} \pm \widehat{U}_X \tag{20}$$

where $\overline{X}$ denotes the nominal value and $\pm\widehat{U}_X$ the uncertainty about the nominal value.

The respective uncertainty in the output parameter $Y(X)$ due to uncertainty in X is given as [92].

$$\widehat{U}_Y = \frac{dY}{dX}\widehat{U}_X \tag{21}$$

For a multi-variate response variable, the total uncertainty is given as [93].

$$\widehat{U}_Y = \left[\sum_{j=1}^{N}\left(\frac{\partial Y}{\partial X_j}\widehat{U}_{Xj}\right)^2\right]^{1/2} \tag{22}$$

Where each partial derivative term in the above equation represents the sensitivity coefficient (SC) of the respective variable [93]. These coefficients are further refined by normalizing the perturbations in the outlet parameter Y and input parameter X by their corresponding nominal values and are known as Normalized Sensitivity Coefficients (NSC) [94]. This normalization allows a comparison of parameters with a significantly different magnitude on a common platform [95]. These coefficients are given mathematically as [96].

$$\frac{\widehat{U}_Y}{\overline{Y}} = \left[\sum_{j=1}^{N}\overbrace{\left(\frac{\partial Y}{\partial X_j}\frac{\overline{X}_j}{\overline{Y}}\right)^2}^{NSC}\overbrace{\left(\frac{\widehat{U}_{Xj}}{\overline{X}_j}\right)^2}^{N\widehat{U}_{Xj}}\right]^{1/2} \tag{23}$$

where NSC is the normalized sensitivity coefficient and the NU is the normalized uncertainty.

In the current analysis, the heat transfer coefficient, pressure drop, operational cost, and stream cost are taken as response parameters. The input variables involve process parameters like mass flow rate, fluid temperature, and monetary parameters i.e., interest rate, energy cost, and cost index factor.

The relative contribution (RC) of the input parameter is another key factor that is used to classify the leading responders to uncertainty by merging the sensitivity coefficients with the actual uncertainties [95]. It is calculated as a square of the product of SC and U, normalized by U^2 of the output parameter [96].

$$RC = \frac{\left(\frac{\partial Y}{\partial X_j}\widehat{U}_{Xj}\right)^2}{\widehat{U}_Y^{\,2}} \tag{24}$$

4. Numerical solution strategy

The above presented mathematical model is numerically solved on Engineering Equation Solver (EES) software. First, the process parameters (i.e., T, P, m, etc.) are provided as input known data (refer to Table 1). Then the thermophysical properties are calculated at inlets and outlets of the pumps and heat exchanger using the seawater library [61]. This is followed by a detailed exergoeconomic analysis. Then the normalized sensitivity analysis is conducted to estimate the NSC and RC of important input parameters. This is followed by the parametric analysis of sensitive input parameters on the comprehensive HX performance. Finally, the Genetic Algorithm is employed for optimization of the geometric parameters for the minimum total cost (C_{total}). The solution flow chart for the numerical code is presented in Fig. 5.

The simulation is based on the following standard assumptions: (a) steady flow process, (b) significant heat transfer in transverse direction only, (c) uniform heat transfer coefficients, (d) insignificant heat loss in and ΔP in pipes, (e) incompressible fluid flow, (f) no heat leak to the environment, (g) constant thermal conductivity of plates, and (h) no endogenous or exogeneous heat sources or sinks other than hot and cold fluids.

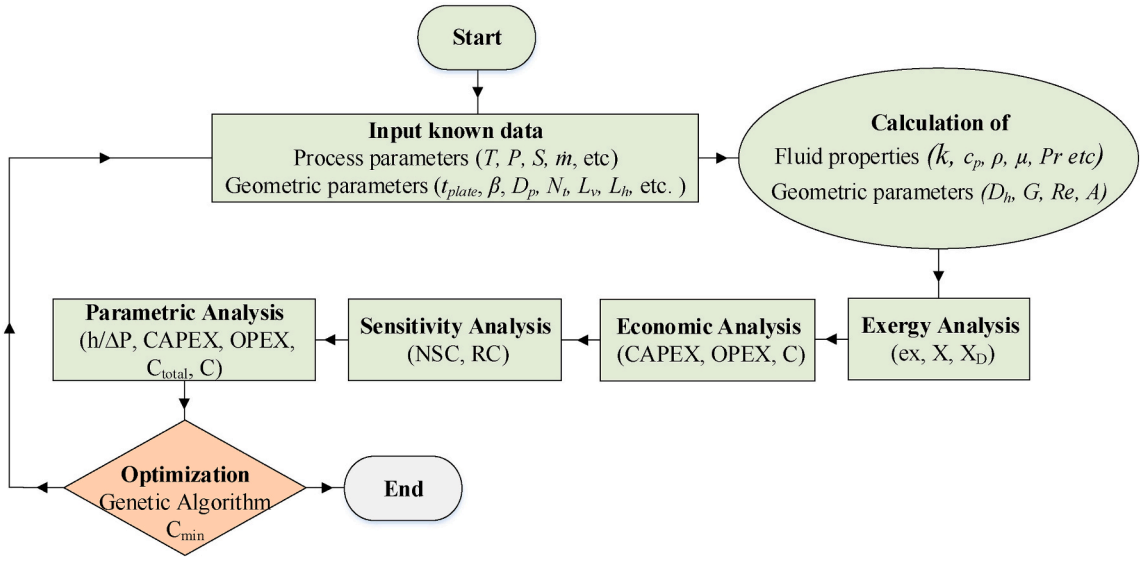

Fig. 5. The simulation flow chart for simulation.

5. Results and discussion

5.1. Model validation

The numerical model developed is validated with the experimental data from a laboratory-scale PHX (Model: edibon-TIPL-0083/16) shown in Fig. 6. The geometric parameters of the experimental setup are presented in the referred study [50]. The experiments are conducted for three different operating scenarios as summarized in Fig. 7. For each case, the setup is operated for 35 min and the data is recorded after the system stabilized. For numerical validation, the recorded data (from the data acquisition system i.e., edibon-SCADA) is imported in EES software using the Look-up table command. Fig. 6 shows a very close agreement between experimental and numerical values. However, at flow rates approaching the maximum operating limits of HX, a deviation (max ±10%) is observed probably due to the inaccuracy of flow sensors and non-negligible heat losses.

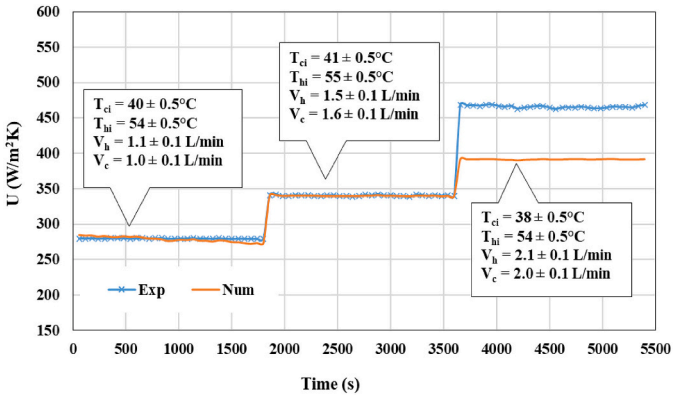

Fig. 7. Model validation with experimental data [50].

5.2. Preliminary design

It involves thermohydraulic design and analysis from an exergy and economic viewpoint as presented in Table 3 also reported by Jamil and Zubair [53]. The initial design reports that an area of 245 m^2 is required to increase the intake seawater temperature from 21 °C to 57 °C by recovering heat from the brine stream entering the HX at 63 °C and leaving at 23 °C. The other thermal-hydraulic performance parameters are calculated as $h_h = 12.2$ kW/m^2K, $h_c = 12.5$ kW/m^2K, $U = 4.9$ kW/m^2K, $\Delta P_h = 48.4$ kPa, $\Delta P_c = 48.1$ kPa, and $PP = 1.55$ kW. Similarly, the

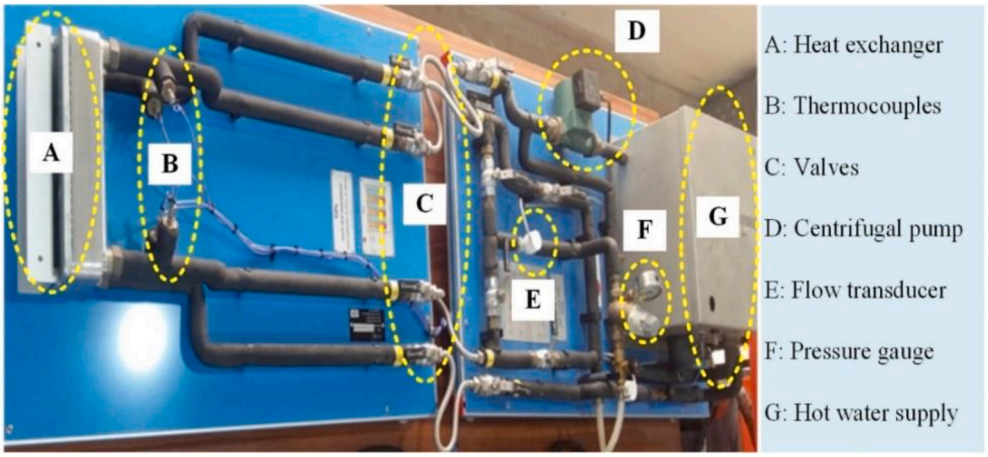

Fig. 6. Experimental test setup.

Table 3
Preliminary analysis of PHX for the MVC system.

Parameters	Value
Chevron angle β, deg	45
Effective heat transfer area A_e, m^2	245
Number of plates, N_p	291
Heat transfer coefficient, h_h / h_c $kW/m^2.K$	12.2 / 12.5
Hot side pressure drop, $\Delta P_{h,Total}$ / $\Delta P_{c,Total}$ kPa	48.4 / 48.12
The ratio of heat transfer coefficient and pressure drop, $h_c/\Delta P_{c,Totab}$ $m/s\ K$	0.26
Overall heat transfer coefficient, U_c, W/m^2K	4968
Pumping power, PP, kW	1.56
Total exergy destruction, $X_{D,Totab}$, kW	32
Heat exchanger capital cost, $CAPEX_{HX}$, $k$$	161
Operational cost, $OPEX$, $k$$	6
Total cost, $Ctotal$, $k$$	167
Stream cost of hot outlet, $\dot{C}_{h,o}/\dot{C}_{c,o}$, $/h	0.52/12.65

exergoeconomic analysis estimated the total exergy destruction as 31.81 kW, the total capital expenses as 164.46 k$, operational expenses as 6 k$, and the stream cost for feed water at the HX outlet as 12.65 $/h.

5.3. Sensitivity analysis

The study is carried out to determine the most influential parameters influencing the output parameters, i.e. the coefficient of heat transfer, pressure drop, operating cost, and stream cost. The results are presented in terms of NSC and RC as shown in Fig. 8. It is seen that (refer to Fig. 8 (a)) The most influential parameters in terms of *NSC* for the heat transfer coefficient (h_c) are the $\dot{m}_c$, followed by $T_{c,\,i}$, andS_c. The corresponding RC is dominated by $\dot{m}_c$with ~88% followed by $T_{c,\,i}$, and S_c with ~11.7% and ~ 0.05%, respectively. Similarly, for pressure drop (ΔP_c) (refer Fig. 8 (b)) the most influential parameter is $\dot{m}_c$ with an RC of ~99.6%.

Likewise, from the economic viewpoint (refer to Fig. 8 (c)), the OPEX appeared to be sensitive to the fiscal parameters in as follows $\dot{m}_c > \dot{m}_h > C_{ele} > i > \eta_p$. While, the RC is the highest for C_{ele} with ~86.2%, followed by i, $\dot{m}_c$, $\dot{m}_h$, and η_p with ~8.94%, ~1.88%, ~1.84%, and ~ 1.15%, respectively. The product cost ($C_{c,o}$) has NSC as follows $C_{index} > i > T_{h,\,i} > \eta_p > \dot{m}_c > \dot{m}_h > C_{ele}$. While, the RC is the highest for i with ~95.5% followed by $C_{index}$and $T_{h,\,i}$ with ~2.50% and ~ 1.65%, respectively as illustrated in Fig. 8 (d).

Overall, the exergoeconomic performance of PHX is sensitive to several processes and fiscal parameters. Therefore, an equivalent apportionment should be given to sensitive parameters while designing/analyzing the heat exchanger.

5.4. Thermal hydraulic and economic

The most influential parameters affecting the heat transfer coefficient (h) and pressure drop (ΔP) of PHXs are mass flow rate and plate chevron angle [50]. The h and ΔP increased with increasing flow rate. However, the pressure drop observed a higher-order increase compared to h. Therefore, the h/ΔP factor reduced with increasing flow rate as

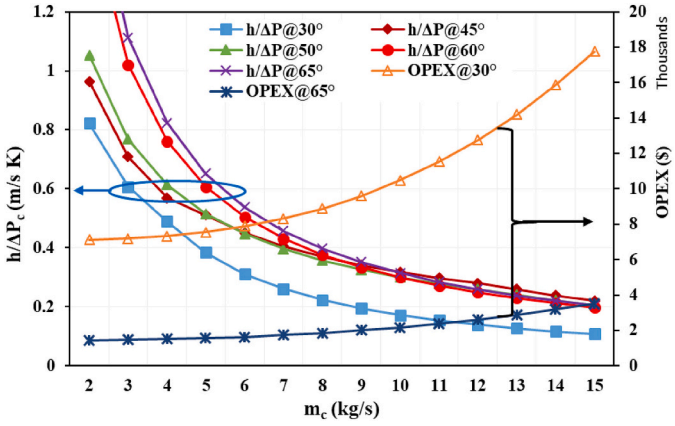

Fig. 9. Effect of flow rate on h/ΔP and operational expenses.

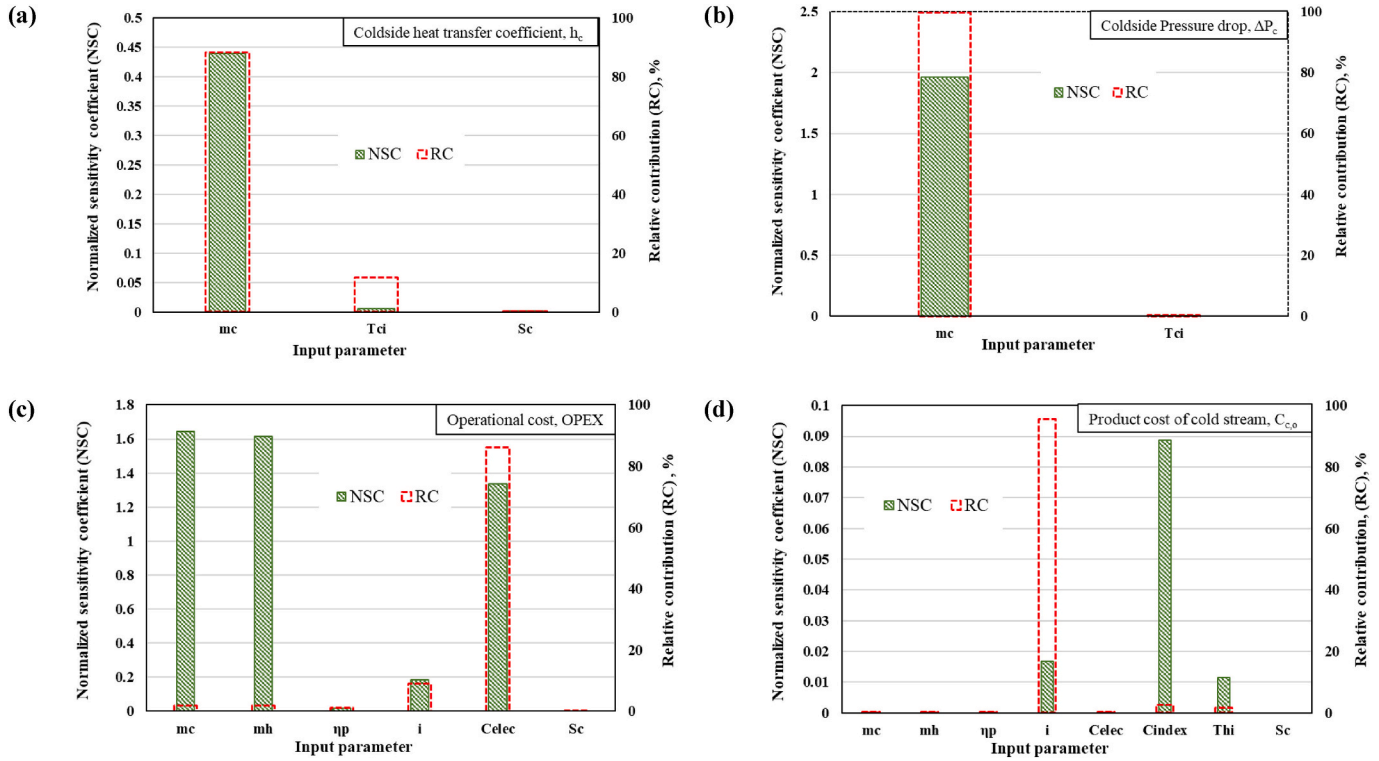

Fig. 8. Sensitivity analysis results i.e., NSC and RC of different input parameters on performance parameters (a) h_c (b) ΔP_c (c) OPEX (d) $C_{c,o}$.

shown in Fig. 9. Similarly, for chevron angle, the h/ΔP followed the order as $\beta = 65^\circ > 60^\circ > 50^\circ > 45^\circ$ with the lowest for $\beta = 30^\circ$ due to very high-pressure drop.

Similarly, the operational cost (OPEX) and outlet cost of the cold stream ($\dot{C}_{c,o}$) increased because the pressure drop is increasing at high order which consumes more pumping power and ultimately the cost of electricity increased as illustrated in Figs. 9 and 10. Thus, for the chevron angle, the OPEX and $\dot{C}_{c,o}$ followed the order as $\beta = 30^\circ > 45^\circ > 50^\circ > 60^\circ$ with the lowest for $\beta = 65^\circ$ due to low-pressure drop at high chevron angle which consumes low pumping power.

5.5. Effect of economic parameters

The conventional studies are primarily targeted at analyzing the effect of the flow and geometric parameters. However, the investigation of the combinatory effect of process and fiscal parameters on the thermo-economics performance gained significant importance in recent studies [23,65]. This is because the system operating with a different inflation rate, the unit cost of electricity, the chemical cost would certainly have different operating costs (OPEX) with similar thermal-hydraulic efficiency [53,66]. As the sensitivity analysis emphasizes in the above section, the importance of influencing economic parameters on the monetary output of PHXThe investigation of the fiscal parameters of PHX's economic output has therefore yielded accurate results for different regions and/or different economic policies over time.

The total cost (C_{total}) and product cost of the cold stream ($\dot{C}_{c,o}$) are increasing as the cost index factor, inflation rate and cost of electricity are increasing as shown in Fig. 10. For instance, for C_{index}= 1.7, $C_{total}$and $\dot{C}_{c,o}$(refer to Fig. 11 (a) and (b)) increased ~62% and ~ 13.85% for β = 30° over 30 years due to market inflation. Similarly, for β = 30°, the $\dot{C}_{c,o}$(refer to Fig. 11 (c) and (d)) increased ~17.7% and ~ 3.80% when the inflate rate and electricity cost varies from 1 to 14% and 0.01–0.15 $/kWh respectively. Therefore, for chevron angle, $C_{total}$and $\dot{C}_{c,o}$ followed the order as $\beta = 30^\circ > 45^\circ > 50^\circ > 60^\circ$ with the lowest for $\beta = 65^\circ$ for the fiscal parameters.

5.6. Exergoeconomic flow diagram

A significant visual representation of the thermo-economic output at each specific point of the system is the exergoeconomic flow diagram. It illustrates the exergy and economics of all streams at the inlet and out of each component of the system calculated using local process and fiscal parameters. The pictorial demonstration is important for multi-component systems to identify how efficiently each component in the system is working from exergetic and economic viewpoints. Contrarily, the simple economic analysis gives the inputs and outputs at system boundaries only. For the current analysis, this diagram is shown in Fig. 12.

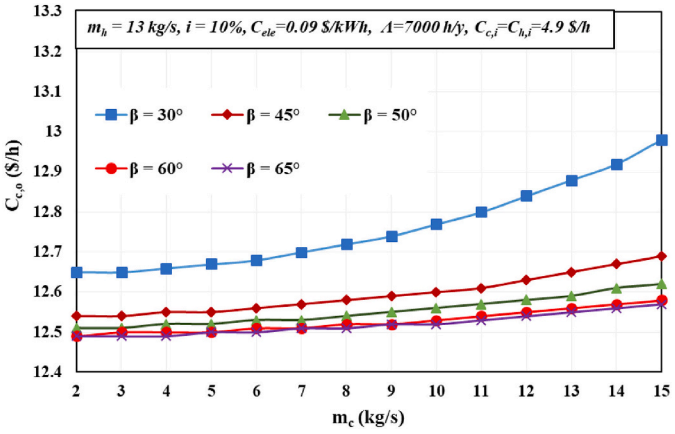

Fig. 10. Effect of feed mass flow rate on the product cost of the cold stream.

6. Optimization

After a detailed normalized sensitivity and parametric analyses, the cost optimization of PHX as a brine preheater of a conventional single effect MVC system as shown in Fig. 13 is conducted. For this purpose, the Genetic Algorithm ie employed such that the total cost (C_{total}) of equipment is taken as an objective function that must be minimized meanwhile maintaining the thermal performance of PHX. The decision parameters against the objective function (C_{total}) are port diameter, the horizontal distance between opening, pitch, tube thickness, enlargement factor, and a number of plates.

The ranges of constrains variables are selected carefully from the literature [49,97] as summarized in Table 4. It is important to mention that the chevron angle (β) is taken as constant for optimization because the chevron angle is the most influential geometric parameters which affect the thermal performance of the heat exchanger [35–39]. Therefore, it's taken as constant to maintain or improve the thermal performance of the heat exchanger [97,98]. The values of algorithm-specific parameters i.e., generations = 400, population size = 150, and mutation probability = 0.035 are taken as reported by Hajabdollahi et al. [49]. The convergence of the genetic algorithm is illustrated in Fig. 14. The perfect convergence has occurred almost within 201 generations (30,475 iterations). However, the C_{total} is reduced by ~52.5% at 50 generations (7677 iterations).

The detailed results of the optimization for PHX via a genetic algorithm (GA) is represented in Table 5. It can be observed that the optimization altered the thermal, hydraulic, and economic performance of PHX. The thermal performance of PHX is improved as the heat transfer of hot and cold streams is increased by ~58.74% and ~ 58.73 respectively which increased the overall heat transfer coefficient by ~65.4%. However, the pressure is high as compared to standard values but within the permissible range of plate heat exchanger i.e., 0.1–1.5 MPa [56]. The comprehensive parameter h/ΔP is reduced by ~46.6% because of pressure drops. The pumping power is also increased by 2.97 folds to overcome the pressure drop across the heat exchanger.

Meanwhile, due to the modification in the design parameters, the number of plates and tube thickness is reduced while the port diameter and tube pitch are increased. The heat transfer area is reduced significantly by~79.5% which reduced the capital investment (CAPEX) by ~62%. Also, the operational cost (OPEX) increased from 6.02 k$ to 17.91 k$ due to pumping power. However, the overall impact is beneficial as the total cost (C_{total}) of the equipment is reduced by ~52.7%. Similarly, the outlet cost of the feed water stream is reduced by ~15.7%.

Overall, the sensitivity analysis and optimization of traditional PHX have greatly enhanced the design and analysis process. Therefore, modern system analysis should be extended to normalized sensitivity analysis and optimization rather than relying exclusively on classical parametric analysis.

7. Concluding remarks

A liquid phase water-to-water plate heat exchanger is investigated as a preheater that uses hot brine coming from a single effect mechanical vapor compression (SEE-MVC) based thermal desalination system. The system is analyzed from thermo-hydraulic, and economic viewpoints. The EES based numerical code is validated against the experimental setup. Sensitivity and parametric analyses are used to investigate the most important parameters. The exergy-and-cost flow-based exergoeconomic analysis is also conducted to calculate the exergies and outlet cost of streams at each component of the system. Finally, the multi-objective optimization of PHX is performed using the Genetic Algorithm. The major findings of the study are as follows.

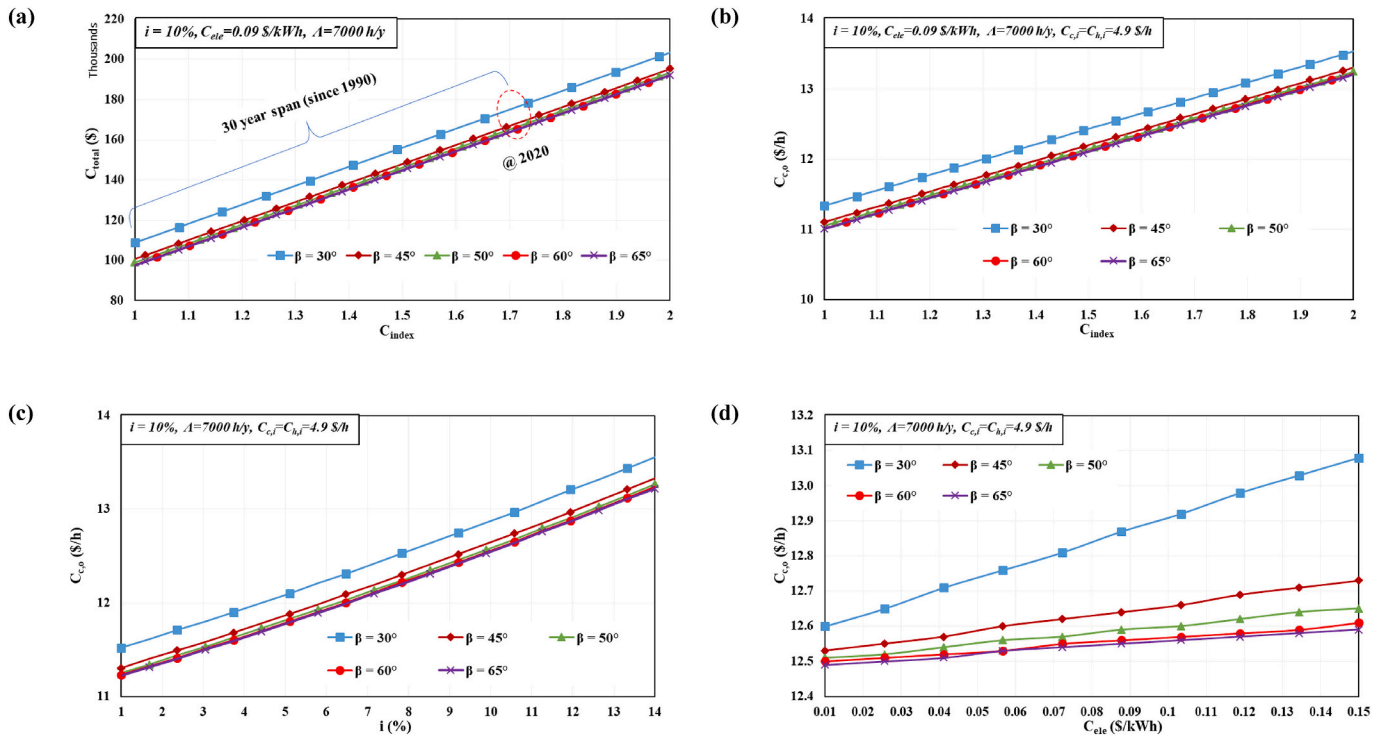

Fig. 11. Effect of monetary (a) total cost against cost index factor, (b) cold water outlet cost against cost index factor, (c) cold water outlet cost against interest rate, and (d) cold water outlet cost against unit electricity cost.

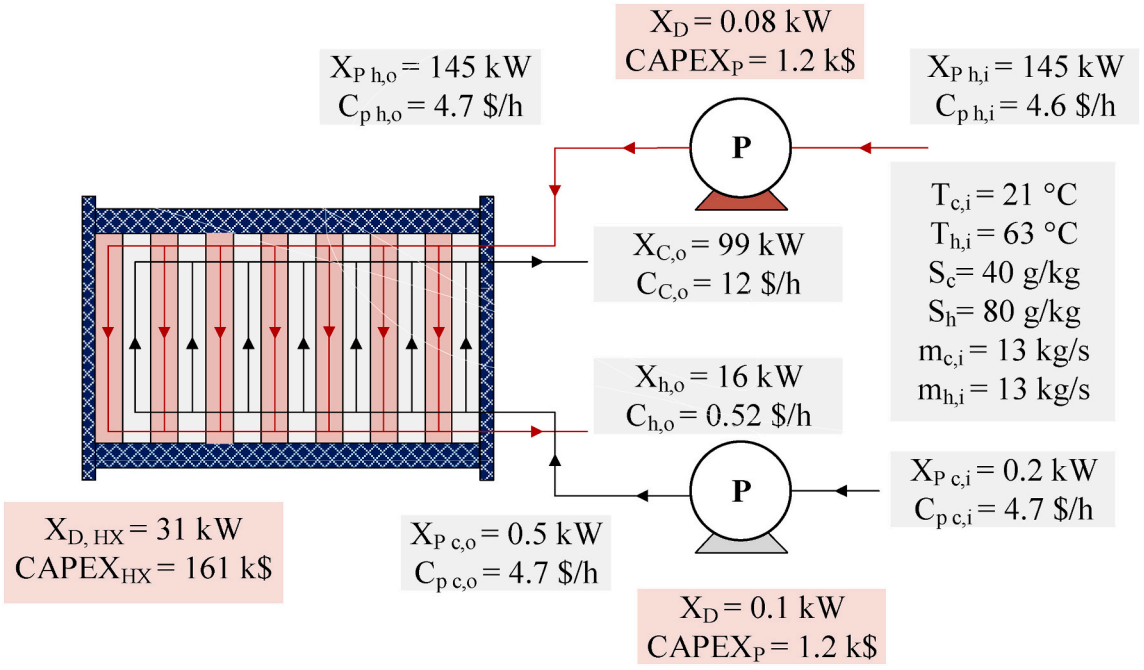

Fig. 12. Exergoeconomic flow diagram for PHX arrangement.

- The normalized sensitivity analysis shows that the most influential parameters in terms of NSC for the heat transfer coefficient (h_c) are the $\dot{m}_c$, followed by $T_{c,\,i}$, and S_c. Similarly, for pressure drop (ΔP_c), the most influential parameter is $\dot{m}_c$. Furthermore, the OPEX appeared to be sensitive to the fiscal and process parameters in the following order $\dot{m}_c > \dot{m}_h > C_{ele} > i > \eta_p$ while the and the product cost ($C_{c,o}$) followed as $C_{index} > i > T_{h,\,i} > \eta_p > \dot{m}_c > \dot{m}_h > C_{ele}$.
- The parametric analysis shows that an increase in the feed mass flow rate decreases h/ΔP because of high order rise in pressure drop but increases the operational cost and outlet cost of the cold stream due to high consumption of pumping power to overcome pressure drop. Therefore, for the chevron angle, the OPEX and $\dot{C}_{c,o}$ followed the order as $\beta = 30° > 45° > 50° > 60°$ with the lowest for $\beta = 65°$ due to low-pressure drop at a high angle which required low power.

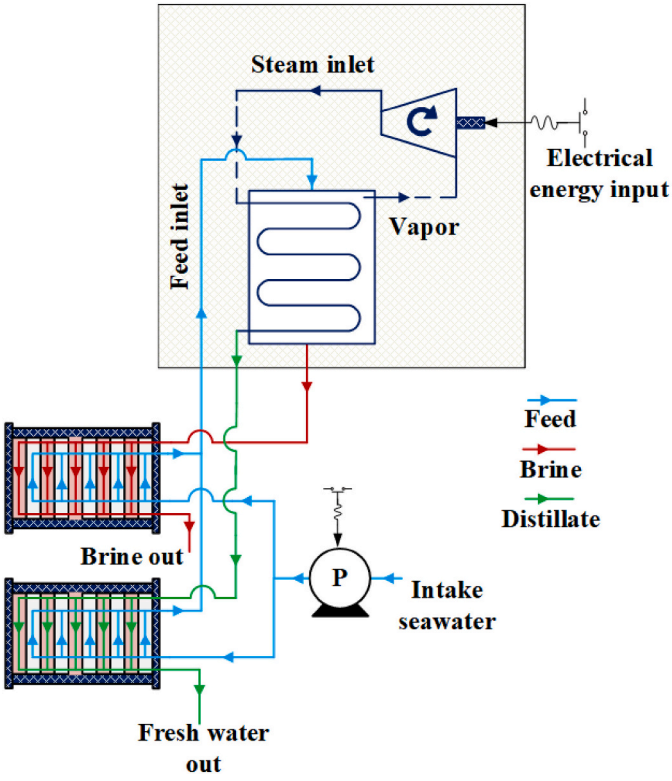

Fig. 13. Single effect MVC system.

Table 4
Values for genetic algorithm [49,97].

Parameters	Guess Values	Constraint bounds		
		Lower	Upper	Optimum[a]
Port diameter, m	0.2	0.1	0.4	0.4
Horizontal distance opening, m	0.43	0.3	0.7	0.3995
Pitch, m	0.001306	0.0010	0.0014	0.0014
Tube thickness, m	0.0006	0.0003	0.003	0.0003
Enlargement factor	1.25	1.15	1.25	1.15
Number of plates	291	50	700	57
Chevron angle, deg	45	Constant		45

Note: Not all references provided all the data ranges.
[a] : Calculated.

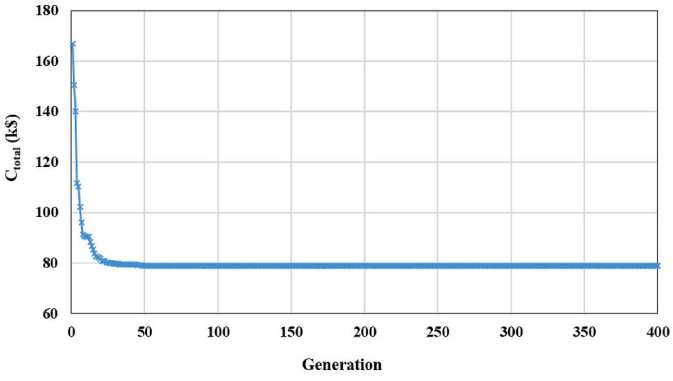

Fig. 14. The convergence of the Genetic Algorithm.

- The fiscal parameters such as unit cost of electricity, inflation rate, and cost index factor have an equivalent effect on the operational cost and outlet cost of PHX compared to the process and design parameters. An increase in C_{ele}, C_{index}, and i increased the operational and outlet cost of the cold stream.
- The GA optimization improved the performance of PHX by modifying the design parameters. The optimum heat exchanger area is reduced by ~79.5%, capital investment by ~62%, and the outlet cost of the cold stream by ~15.7%. The operational cost is increased from 6.02 k$ to 17.91 k$ due to increased pressure drop. However, the overall impact is beneficial as $C_{total}$is reduced by ~52.7%.

Table 5
Optimization results for PHX using GA.

Parameters	SEE-MVC	
	Standard	**Optimal**
Chevron angle, β, *deg*	45	45*
Effective heat transfer area, A_e, m^2	246	50 ↓
Number of plates, N_p	291	57 ↓
Hot side heat transfer coefficient, h_h, $kW/m^2.K$	12	19 ↑
Cold side heat transfer coefficient, h_c, kW/m^2K	12	19↑
Hot side pressure drop, $\Delta P_{h,Totab}$, *kPa*	48	144 ↑
Cold side pressure drop, $\Delta P_{c,Total}$, *kPa*	48	143 ↑
Cold side $h_c/\Delta P_{c,Total}$, *m/s K*	0.26	0.14 ↓
Overall Heat transfer coefficient U_c, kW/m^2K	5	8 ↑
Pumping power, *PP, kW*	1.56	4.63↑
Total exergy destruction, $X_{D,Total}$, *kW*	32	35 ↑
Heat exchanger capital expenses, $CAPEX_{HX}$, *k$*	161	61↓
Total capital expenses, $CAPEX_{Total}$, *k$*	164	67 ↓
Operational expenses, *OPEX, k$*	6	17 ↑
Total cost, C_{total}, *k$*	167	79 ↓
Brine outlet stream cost, $\dot{C}_{h,o}$, *$/h*	0.52	0.53 ↑
Feed outle stream cost, $\dot{C}_{c,o}$, *$/h*	12.65	10.66 ↓

↓: Decrease, ↑: Increase, *: Same.

Author contributions

Muhammad Ahmad Jamil, Muhammad Wakil Shahzad and Kim Choon Ng proposed the idea and developed overall methodology. Talha S. Goraya, Ben Bin Xu and Syed M. Zubair collected data, developed detailed simulation and conducted detailed analysis. Muhammad Ahmad Jamil, Muhammad Wakil Shahzad developed detailed optimization technique. Muhammad Ahmad Jamil prepared the initial draft. Muhammad Wakil Shahzad reviewed the manuscript. Kim Choon Ng and Syed M. Zubair prepared the final draft.

Declaration of Competing Interest

The authors declare that they have no known competing financial interests or personal relationships that could have appeared to influence the work reported in this paper.

The authors declare the following financial interests/personal relationships which may be considered as potential competing interests:

Acknowledgment

The authors acknowledge the support provided by Northumbria University, UK under reference # RDF20/EE/MCE/SHAHZAD and MCE QR funds 2020/21. Ben Xu would like to thank the support from EPSRC grants EP/N007921/1.

References

[1] M.W. Shahzad, M. Burhan, D. Ybyraiymkul, K.C. Ng, Desalination processes' efficiency and future roadmap, Entropy 21 (2019).
[2] Y. Junjie, S. Shufeng, W. Jinhua, L. Jiping, Improvement of a multi-stage flash seawater desalination system for cogeneration power plants, Desalination 217 (2007) 191–202.
[3] B. Najafi, A. Shirazi, M. Aminyavari, F. Rinaldi, R.A. Taylor, Exergetic, economic and environmental analyses and multi-objective optimization of an SOFC-gas turbine hybrid cycle coupled with an MSF desalination system, Desalination 334 (2014) 46–59.

[4] R. Kouhikamali, S.M.A. Noori Rahim Abadi, M. Hassani, Numerical investigation of falling film evaporation of multi-effect desalination plant, Appl. Therm. Eng. 70 (2014) 477–485, https://doi.org/10.1016/j.applthermaleng.2014.05.039.
[5] K.H. Mistry, M.A. Antar, V.J.H. Lienhard, An improved model for multiple effect distillation, Desalin. Water Treat. 51 (2013) 1–15.
[6] K.A. Khalid, M.A. Antar, A. Khalifa, O.A. Hamed, Allocation of thermal vapor compressor in multi effect desalination systems with different feed configurations, Desalination 426 (2018) 164–173.
[7] D. Han, W.F. He, C. Yue, W.H. Pu, Study on desalination of zero-emission system based on mechanical vapor compression, Appl. Energy 185 (2017) 1490–1496.
[8] K. Thu, A. Chakraborty, Y.D. Kim, A. Myat, B.B. Saha, K.C. Ng, Numerical simulation and performance investigation of an advanced adsorption desalination cycle, Desalination 308 (2013) 209–218, https://doi.org/10.1016/j.desal.2012.04.021.
[9] M.W. Shahzad, K. Choon Ng, K. Thu, B.B. Saha, Multi effect desalination and adsorption desalination (MEDAD): a hybrid desalination method, Appl. Therm. Eng. 72 (2014) 289–297, https://doi.org/10.1016/j.applthermaleng.2014.03.064.
[10] K. Thu, H. Yanagi, B.B. Saha, K.C. Ng, Performance analysis of a low-temperature waste heat-driven adsorption desalination prototype, Int. J. Heat Mass Transf. 65 (2013) 662–669, https://doi.org/10.1016/j.ijheatmasstransfer.2013.06.053.
[11] H.R. Datsgerdi, H.T. Chua, Thermo-economic analysis of low-grade heat driven multi-effect distillation based desalination processes, Desalination 448 (2018) 36–48.
[12] N. Chitgar, M.A. Emadi, A. Chitsaz, M.A. Rosen, Investigation of a novel multigeneration system driven by a SOFC for electricity and fresh water production, Energy Convers. Manag. 196 (2019) 296–310.
[13] M.W. Shahzad, K. Thu, Y. Kim, K.C. Ng, An experimental investigation on MEDAD hybrid desalination cycle, Appl. Energy 148 (2015) 273–281.
[14] M.L. Elsayed, O. Mesalhy, R.H. Mohammed, L.C. Chow, Exergy and thermo-economic analysis for MED-TVC desalination systems, Desalination 447 (2018) 29–42.
[15] M.L. Elsayed, O. Mesalhy, R.H. Mohammed, L.C. Chow, Transient and thermo-economic analysis of MED-MVC desalination system, Energy 167 (2019) 283–296.
[16] Z. Zhang, S. Sridhar, G. Wei, Y. Yu, Z. Zhang, L. Jiang, et al., Surface & Coatings Technology a highly controlled fabrication of porous anodic aluminium oxide surface with versatile features by spatial thermo-anodization, Surf. Coat. Technol. 408 (2021) 126809, https://doi.org/10.1016/j.surfcoat.2020.126809.
[17] A.S. Nafey, H.E.S. Fath, A.A. Mabrouk, Thermo-economic investigation of multi effect evaporation (MEE) and hybrid multi effect evaporation-multi stage flash (MEE-MSF) systems, Desalination 201 (2006) 241–254.
[18] H.M. Ettouney, H.T. El-Dessouky, R.S. Faibish, P.J. Gowin, Evaluating the economics of desalination, Chem. Eng. Process. 98 (1986) 32–39.
[19] A.A. Mabrouk, A.S. Nafey, H.E.S. Fath, Thermoeconomic analysis of some existing desalination processes, Desalination 205 (2007) 354–373.
[20] A.S. Nafey, H.E.S. Fath, A.A. Mabrouk, Thermoeconomic design of a multi-effect evaporation mechanical vapor compression (MEE – MVC) desalination process, Desalination 230 (2008) 1–15.
[21] Y. Zhang, H. Zhang, W. Zheng, S. You, Y. Wang, Numerical investigation of a humidification-dehumidification desalination system driven by heat pump, Energy Convers. Manag. 180 (2019) 641–653.
[22] G.F. Hewitt, G.L. Shires, T.R. Bott, Process Heat Transfer, CRC, New York, 1994.
[23] M.A. Jamil, S.M. Zubair, Design and analysis of a forward feed multi-effect mechanical vapor compression desalination system: an exergo-economic approach, Energy 140 (2017) 1107–1120.
[24] M.A. Darwish, M.A. Jawad, G.S. Aly, Comparison between small capacity mechanical vapor compression (MVC) and reverse osmosis (RO) desalting plants, Desalination 78 (1990) 313–326.
[25] Y. Zhou, C. Shi, G. Dong, Analysis of a mechanical vapor recompression wastewater distillation system, Desalination 353 (2014) 91–97.
[26] N.H. Aly, A.K. El-Fiqi, Mechanical vapor compression desalination systems - a case study, Desalination 158 (2003) 143–150.
[27] M.L. Elsayed, O. Mesalhy, R.H. Mohammed, L.C. Chow, Transient performance of MED processes with different feed configurations, Desalination 438 (2018) 37–53.
[28] H. Ettouney, Design of single-effect mechanical vapor compression, Desalination 190 (2006) 1–15.
[29] H. El-Dessouky, H.M. Ettouney, S. Bingulac, I. Alatiqi, Steady-state analysis of the multiple effect evaporation desalination process, Chem. Eng. Technol. 21 (1998) 437–451.
[30] H.M. Ettouney, H.T. El-Dessouky, Fundamentals of Salt Water Desalination, 2002.
[31] H.T. El-Dessouky, H.M. Ettouney, Y. Al-roumi, Multi-stage flash desalination : present and future outlook, Chem. Eng. J. 73 (1999) 173–190.
[32] A. Lozano, F. Barreras, N. Fueyo, S. Santodomingo, The flow in an oil / water plate heat exchanger for the automotive industry, Appl. Therm. Eng. 28 (2008) 1109–1117, https://doi.org/10.1016/j.applthermaleng.2007.08.015.
[33] C. Gulenoglu, F. Akturk, S. Aradag, N.S. Uzol, S. Kakac, Experimental comparison of performances of three different plates for gasketed plate heat exchangers, Int. J. Therm. Sci. 75 (2014) 249–256, https://doi.org/10.1016/j.ijthermalsci.2013.06.012.
[34] L.E. Dodd, D. Wood, N.R. Geraldi, G.G. Wells, G. Mchale, B.B. Xu, et al., Low friction droplet transportation on a substrate with a selective Leidenfrost E ff ect, Appl. Mater. Interfaces 8 (2016) 22658–22663, https://doi.org/10.1021/acsami.6b06738.
[35] K. Sarraf, S. Launay, L. Tadrist, Complex 3D-flow analysis and corrugation angle effect in plate heat exchangers, Int. J. Therm. Sci. 94 (2015) 126–138, https://doi.org/10.1016/j.ijthermalsci.2015.03.002.
[36] O. Giurgiu, A. Pleșa, L. Socaciu, Plate heat exchangers - flow analysis through mini channels, Energy Procedia 85 (2016) 244–251, https://doi.org/10.1016/j.egypro.2015.12.236.
[37] B. Kumar, A. Soni, S.N. Singh, Effect of geometrical parameters on the performance of chevron type plate heat exchanger, Exp. Thermal Fluid Sci. 91 (2018) 126–133, https://doi.org/10.1016/j.expthermflusci.2017.09.023.
[38] C. Turk, S. Aradag, S. Kakac, Experimental analysis of a mixed-plate gasketed plate heat exchanger and artificial neural net estimations of the performance as an alternative to classical correlations, Int. J. Therm. Sci. 109 (2016) 263–269, https://doi.org/10.1016/j.ijthermalsci.2016.06.016.
[39] K. Nilpueng, T. Keawkamrop, H.S. Ahn, S. Wongwises, Effect of chevron angle and surface roughness on thermal performance of single-phase water flow inside a plate heat exchanger, Int Commun Heat Mass Transf 91 (2018) 201–209, https://doi.org/10.1016/j.icheatmasstransfer.2017.12.009.
[40] B.H. Shon, C.W. Jung, O.J. Kwon, C.K. Choi, Y.T. Kang, Characteristics on condensation heat transfer and pressure drop for a low GWP refrigerant in brazed plate heat exchanger, Int. J. Heat Mass Transf. 122 (2018) 1272–1282, https://doi.org/10.1016/j.ijheatmasstransfer.2018.02.077.
[41] R. Eldeeb, V. Aute, R. Radermacher, A survey of correlations for heat transfer and pressure drop for evaporation and condensation in plate heat exchangers, Int. J. Refrig. 65 (2016) 12–26, https://doi.org/10.1016/j.ijrefrig.2015.11.013.
[42] R.L. Amalfi, F. Vakili-Farahani, J.R. Thome, Flow boiling and frictional pressure gradients in plate heat exchangers. Part 1: review and experimental database, Int. J. Refrig. 61 (2016) 166–184, https://doi.org/10.1016/j.ijrefrig.2015.07.010.
[43] J.A.W. Gut, J.M. Pinto, Optimal configuration design for plate heat exchangers, Int. J. Heat Mass Transf. 47 (2004) 4833–4848, https://doi.org/10.1016/j.ijheatmasstransfer.2004.06.002.
[44] M. Yildirim, M.S. Söylemez, Thermo economical optimization of plate type of heat exchangers for waste heat recovery, J. Therm. Sci. Technol. 36 (2016) 57–60.
[45] F. Hajabdollahi, Z. Hajabdollahi, H. Hajabdollahi, Optimum design of gasket plate heat exchanger using multimodal genetic algorithm, Heat Transf. Res. 44 (2013) 761–789, https://doi.org/10.1615/HeatTransRes.2013006366.
[46] N.R. Geraldi, L.E. Dodd, B.B. Xu, G.G. Wells, D. Wood, M.I. Newton, et al., Drag reduction properties of superhydrophobic mesh pipes, Surf. Topogr Metrol. Prop. Pap. 5 (2017), 034001.
[47] O. Arsenyeva, L. Tovazhnyansky, P. Kapustenko, G. Khavin, Mathematical modelling and optimal design of plate-and-frame heat exchangers, Chem. Eng. Trans. vol. 18 (2009) 791–796, https://doi.org/10.3303/CET0918129. Italian Association of Chemical Engineering - AIDIC.
[48] O.P. Arsenyeva, L.L. Tovazhnyansky, P.O. Kapustenko, G.L. Khavin, Optimal design of plate-and-frame heat exchangers for ef fi cient heat recovery in process industries, Energy 36 (2011) 4588–4598, https://doi.org/10.1016/j.energy.2011.03.022.
[49] H. Hajabdollahi, M. Naderi, S. Adimi, A comparative study on the shell and tube and gasket-plate heat exchangers: the economic viewpoint, Appl. Therm. Eng. 92 (2016) 271–282.
[50] M.A. Jamil, Z.U. Din, T.S. Goraya, H. Yaqoob, S.M. Zubair, Thermal-hydraulic characteristics of gasketed plate heat exchangers as a preheater for thermal desalination systems, Energy Convers. Manag. 205 (2020) 112425.
[51] A. Abid, Exergoeconomic Analysis of Single and Multi-Effect Desalination Systems, MS Thesis, Khwaja Fareed University of Engineering and Information Technology Rahim Yar Khan, Department of Mechanical Engineering, 2020.
[52] A. Abid, M.A. Jamil, Sabah N. Us, M.U. Farooq, H. Yaqoob, L.A. Khan, et al., Exergoeconomic optimization of a forward feed multi-effect desalination system with and without energy recovery, Desalination 499 (2020) 114808, https://doi.org/10.1016/j.desal.2020.114808.
[53] M.A. Jamil, S.M. Zubair, On thermoeconomic analysis of a single-effect mechanical vapor compression desalination system, Desalination 420 (2017) 292–307.
[54] A.K. Tiwari, P. Ghosh, J. Sarkar, Performance comparison of the plate heat exchanger using different nanofluids, Exp. Thermal Fluid Sci. 49 (2013) 141–151, https://doi.org/10.1016/j.expthermflusci.2013.04.012.
[55] B.D. Raja, R.L. Jhala, V. Patel, Thermal-hydraulic optimization of plate heat exchanger: a multi-objective approach, Int. J. Therm. Sci. 124 (2018) 522–535, https://doi.org/10.1016/j.ijthermalsci.2017.10.035.
[56] S. Kakac, H. Liu, Heat Exchangers: Selection, Rating, and Thermal Design, 2nd ed., CRC, New York, 2002.
[57] M.A. Khairul, M.A. Alim, I.M. Mahbubul, R. Saidur, A. Hepbasli, A. Hossain, Heat transfer performance and exergy analyses of a corrugated plate heat exchanger using metal oxide nanofluids, Int Commun Heat Mass Transf 50 (2014) 8–14, https://doi.org/10.1016/j.icheatmasstransfer.2013.11.006.
[58] Y. Demirel, Thermodynamic analysis of separation systems, Sep. Sci. Technol. 6395 (2010) 3897–3942.
[59] K.H. Mistry, R.K. McGovern, G.P. Thiel, E.K. Summers, S.M. Zubair, V.J. H. Lienhard, Entropy generation analysis of desalination technologies, Entropy 13 (2011) 1829–1864.
[60] M.H. Sharqawy, V.J.H. Lienhard, S.M. Zubair, Thermophysical properties of seawater: a review of existing correlations and data, Desalin. Water Treat. 16 (2010) 354–380.
[61] K.G. Nayar, M.H. Sharqawy, L.D. Banchik, V.J.H. Lienhard, Thermophysical properties of seawater: a review and new correlations that include pressure dependence, Desalination 390 (2016) 1–24.
[62] A.C. Caputo, P.M. Pelagagge, P. Salini, Heat exchanger design based on economic optimisation, Appl. Therm. Eng. 28 (2008) 1151–1159.
[63] H. Sadeghzadeh, M.A. Ehyaei, M.A. Rosen, Techno-economic optimization of a shell and tube heat exchanger by genetic and particle swarm algorithms, Energy

Convers. Manag. 93 (2015) 84–91, https://doi.org/10.1016/j.enconman.2015.01.007.
[64] V.H. Iyer, S. Mahesh, R. Malpani, M. Sapre, A.J. Kulkarni, Adaptive Range Genetic Algorithm: a hybrid optimization approach and its application in the design and economic optimization of Shell-and-Tube Heat Exchanger, Eng. Appl. Artif. Intell. 85 (2019) 444–461, https://doi.org/10.1016/j.engappai.2019.07.001.
[65] M.A. Jamil, S.M. Elmutasim, S.M. Zubair, Exergo-economic analysis of a hybrid humidification dehumidification reverse osmosis (HDH-RO) system operating under different retrofits, Energy Convers. Manag. 158 (2018) 286–297.
[66] M.A. Jamil, S.M. Zubair, Effect of feed flow arrangement and number of evaporators on the performance of multi-effect mechanical vapor compression desalination systems, Desalination 429 (2018) 76–87.
[67] Y.M. El-Sayed, The Thermoeconomics of Energy Conversions, Elsevier, Amsterdam, 2003.
[68] Y.M. El-Sayed, Designing desalination systems for higher productivity, Desalination 134 (2001) 129–158.
[69] A.C. Caputo, P.M. Pelagagge, P. Salini, Manufacturing cost model for heat exchangers optimization, Appl. Therm. Eng. 94 (2016) 513–533, https://doi.org/10.1016/j.applthermaleng.2015.10.123.
[70] C. Zhang, C. Liu, S. Wang, X. Xu, Q. Li, Thermo-economic comparison of subcritical organic Rankine cycle based on different heat exchanger configurations, Energy 123 (2017) 728–741, https://doi.org/10.1016/j.energy.2017.01.132.
[71] J. Li, Z. Yang, S. Hu, F. Yang, Y. Duan, Effects of shell-and-tube heat exchanger arranged forms on the thermo-economic performance of organic Rankine cycle systems using hydrocarbons, Energy Convers. Manag. 203 (2020) 112248, https://doi.org/10.1016/j.enconman.2019.112248.
[72] Y.R. Li, M.T. Du, C.M. Wu, S.Y. Wu, C. Liu, J.L. Xu, Economical evaluation and optimization of subcritical organic Rankine cycle based on temperature matching analysis, Energy 68 (2014) 238–247.
[73] S. Fettaka, J. Thibault, Y. Gupta, Design of shell-and-tube heat exchangers using multiobjective optimization, Int. J. Heat Mass Transf. 60 (2013) 343–354.
[74] W.M. Vatavuk, Updating the cost index, Chem. Eng. (2002) 62–70.
[75] S. Jenkins, Chemical engineering plant cost index annual average, 2019, p. 2020. https://www.chemengonline.com/2019-chemical-engineering-plant-cost-index-annual-average/ (accessed April 9, 2020).
[76] W. El-Mudir, M. El-Bousiffi, S. Al-Hengari, Performance evaluation of a small size TVC desalination plant, Desalination 165 (2004) 269–279.
[77] C. Haslego, G. Polley, Compact heat exchanger-part 1: designing plate-and-frame heat exchangers, CEP Mag (2002) 32–37.
[78] A. Christ, B. Rahimi, K. Regenauer-Lieb, H.T. Chua, Techno-economic analysis of geothermal desalination using hot sedimentary aquifers: a pre-feasibility study for Western Australia, Desalination 404 (2017) 167–181.
[79] B. Rahimi, Z. Marvi, A.A. Alamolhoda, M. Abbaspour, H.T. Chua, An industrial application of low-grade sensible waste heat driven seawater desalination: a case study, Desalination 470 (2019) 114055.
[80] M. Taal, I. Bulatov, J. Kleme, P. Stehl, Cost estimation and energy price forecasts for economic evaluation of retrofit projects, Appl. Therm. Eng. 23 (2003) 1819–1835.
[81] S.G. Hall, S. Ahmad, R. Smith, Capital cost targets for heat exchanger networks comprising mixed materials of construction, pressure ratings and exchanger types, Comput. Chem. Eng. 14 (1990) 319–335.
[82] R.S. El-Emam, I. Dincer, Thermodynamic and thermoeconomic analyses of seawater reverse osmosis desalination plant with energy recovery, Energy 64 (2014) 154–163.
[83] A.S. Nafey, M.A. Sharaf, L. Garcia-Rodriguez, Thermo-economic analysis of a combined solar organic Rankine cycle-reverse osmosis desalination process with different energy recovery configurations, Desalination 261 (2010) 138–147.
[84] A. Lazzaretto, G. Tsatsaronis, SPECO: a systematic and general methodology for calculating efficiencies and costs in thermal systems, Energy 31 (2006) 1257–1289.
[85] M. Rosen, A concise review of exergy-based cconomic methods, Int. Conf. Energy Environ. (2008) 9.
[86] M. Esen, T. Yuksel, Experimental evaluation of using various renewable energy sources for heating a greenhouse, Energy Build 65 (2013) 340–351.
[87] B.A. Qureshi, S.M. Zubair, A comprehensive design and rating study of evaporative coolers and condensers. Part II. Sensitivity analysis, Int. J. Refrig. 29 (2006) 659–668.
[88] J.F. Kitchell, D.J. Stewart, D. Weininger, Applications of a bioenergetics model to yellow perch (Perca flavescens) and walleye (Stizostedion vitreum vitreum), J. Fish. Res. Board Can. 34 (1977) 1922–1935.
[89] H. Esen, M. Inalli, M. Esen, A techno-economic comparison of ground-coupled and air-coupled heat pump system for space cooling, Build. Environ. 42 (2007) 1955–1965.
[90] H. Esen, M. Inalli, M. Esen, Technoeconomic appraisal of a ground source heat pump system for a heating season in eastern Turkey, Energy Convers. Manag. 47 (2006) 1281–1297.
[91] I.S. Hussaini, S.M. Zubair, M.A. Antar, Area allocation in multi-zone feedwater heaters, Energy Convers. Manag. 48 (2007) 568–575, https://doi.org/10.1016/j.enconman.2006.06.003.
[92] J.H. Kim, T.W. Simon, Journal of heat transfer policy on reporting uncertainties in experimental measurements and results, J. Heat Transf. 115 (1993) 5–6, https://doi.org/10.1115/1.2910670.
[93] B.N. Taylor, C.E. Kuyatt, Guidelines for Evaluating and Expressing the Uncertainty of NIST Measurement Results, Gaithersburg, MD, U.S. Departmente of Commerce, Technology Administration, National Institute of Standards and Technology, 1994.
[94] M. Masi, S. Fogliani, S. Carrà, Sensitivity analysis on indium phosphide liquid encapsulated Czochralski growth, Cryst. Res. Technol. 34 (1999) 1157–1167.
[95] C.A. James, R.P. Taylor, B.K. Hodge, The application of uncertainty analysis to cross-flow heat exchanger performance predictions, Heat Transf. Eng. 16 (1995) 50–62.
[96] C.A. James, R.P. Taylor, B.K. Hodge, Analysis and Design of Energy Systems, 3rd ed., Prentice Hall, Englewood Cliffs, NJ, 1998.
[97] H. Najafi, B. Najafi, Multi-objective optimization of a plate and frame heat exchanger via genetic algorithm, 2010, pp. 639–647, https://doi.org/10.1007/s00231-010-0612-8.
[98] M. Imran, N.A. Pambudi, M. Faroq, Thermal-hydraulic optimization of plate heat exchanger using genetic algorithm, Case Stud. Therm. Eng. (2017), https://doi.org/10.1016/j.csite.2017.10.003.